DISTRIBUTION STATEMENT A. Approved for public release; distribution is unlimited.

Shallow Turbulence in Rivers and Estuaries

Stefan A. Talke
Civil and Environmental Engineering Department, Portland State University
PO Box 751-CEE
Portland, OR 97207-0751
phone: (503) 725-2870 fax: (530) 725-4282 email: s.a.talke@pdx.edu

Edward D. Zaron
Civil and Environmental Engineering Department, Portland State University
PO Box 751-CEE
Portland, OR 97207-0751
phone: (503) 725-2435 fax: (530) 725-4282 email: zaron@cecs.pdx.edu

Chris Chickadel
Applied Physics Lab, University of Washington
1013 NE 40th St
Seattle, WA, 98105
phone: (206) 7221-7673 fax: (206) 543-6785 email: chickadel@apl.washington.edu

Award Number: N00014-12-1-0218, N00014-12-1-0219

LONG-TERM GOALS

The overall goal of the "Shallow Turbulence in Rivers and Estuaries" project, from Mar. 2012- Mar. 2014, was to improve our understanding of turbulent mixing processes, dispersion, and energy dissipation in estuaries and rivers, with a focus on eddying motion occurring at horizontal length scales greater than the water depth, and their interaction with bottom boundary turbulence. Our study also aimed to find and better interpret remotely-sensed signatures. Remotely sensed flow and turbulence properties we have found can be used in the future to (a) calibrate models, (b) characterize the skill of predictions, and (c) constrain/estimate important boundary conditions such as river flow or bottom friction.

OBJECTIVES

The objectives of the "Shallow Turbulence in Rivers and Estuaries" project were to analyze and compare existing field data, remotely sensed data, and Delft3D numerical data for evidence of large scale, quasi-2D eddies that are much larger than the depth. Specific objectives were to:

1. *Detect spatial patterns of shallow turbulence from in-situ and remote sensing data;*
2. *Elucidate shallow turbulence properties, statistics, and processes through data analysis and numerical modeling studies; and*
3. *Investigate and synthesize shallow turbulence processes and their interaction with bottom boundary processes*

APPROACH

Our approach combined 1) analysis of existing data, 2) evaluation of new data collected for related projects during the award period and 3) numerical modeling to study the dynamics and significance of shallow turbulence in rivers and estuaries. Infra-red images and surface currents from the Snohomish River, WA (see Chickadel et al., 2011), the New-River Inlet, and the Columbia River (RIVET-II experiment, 2013) have been analyzed. In-situ flow data from the Snohomish River (Talke et al., 2013) and "Mega-Transect data" from the Columbia River mouth (Moritz et al., 2005) has been compared to remote sensing data and modeling results, respectively. CODAR velocity data from http://cencalcurrents.org/DataRealTime/Totals/SF_Bay/ of central San Francisco Bay was also analyzed. Available since 2009, the CODAR data provides surface velocity at 400m resolution over a grid of 11x11 km. The Delft3D modeling system was used to simulate the Columbia River Estuary (CRE), with a focus on analyzing large-scale, horizontal eddying motions. Our analysis strategy consisted of (a) identifying and characterizing large scale 2D eddies, and (b) analyzing 2D and 3D (bottom boundary layer, BBL) flow dynamics and turbulence statistics. The turbulent flow field is found by removing tidal and tidally-averaged flow components through harmonic analysis. Vector plots, vorticity maps, and swirl analysis are then used to detect coherent eddying motion (Zhou et al., 1996, 1999, and Adrian et al, 2000). The integral length scale L_I and TKE are also calculated and a 'dissipation'-like value is estimated via the K-epsilon turbulence model: $\epsilon = \frac{(TKE)^{3/2}}{L_I}$.

In June 2013, surface temperature imagery and Lidar elevation data were collected upstream of the mouth of Columbia River inlet using the APL (Applied Physics Laboratory) airborne remote sensing system. Thermal imagery was collected from uncooled cameras on board the plane in a nadir (downward) pointing geometry to minimize the reflected background radiance. Images were recorded from an altitude of 300m yielding image footprints of 210m x 150m, and 35cm resolution. Simultaneous data of surface velocity and temperature, from ATI SAR (G. Farquharson, APL) and IR sensing respectively, was also collected during the RIVET-II experiment at the Columbia River mouth.

WORK COMPLETED

We have (a) further analyzed and clarified the interpretation of in-situ and surface turbulence from the Snohomish River (Talke); (b) updated the bathymetry and grid of our Columbia River Delft3D model to include flood plains, secondary channels, and all large-scale pile dikes (Talke & Zaron); (c) trained a student to run and analyze sensitivity studies of the Columbia River estuary (CRE) using different roughness and grid conditions (Talke & Zaron); (d) processed and analyzed CODAR data from Central San Francisco Bay (SFB), to gain insights on large-scale turbulence for different river flow conditions (Talke); (e) processed CRE and New River Inlet surface IR data to look for shallow turbulence signatures (Chickadel) ; (f); evaluated flow data from east coast estuaries to find shallow turbulence signatures (Talke; data from Areté Associates; Anderson & Dugan, 2011) (g) processed both in-situ and remote sensing data of the Columbia River Estuary (Zaron & Chickadel). A peer-reviewed manuscript analyzing turbulence in the Snohomish River was published (Talke et al., 2013) and two manuscripts are in preparation (Zaron, Talke). A book chapter containing results from the COHSTREX experiment was published (Jessup et al., 2013), as was a conference paper (Zaron). Results from previous fiscal years are discussed more thoroughly in the 2012 and 2013 Annual Reports (e.g., New River Inlet and Areté data) and Talke et al., 2013; here we focus on work completed since Sept. 2013.

RESULTS

In a tidal river, we find that the largest, energy containing scales are quasi-2D structures which are much larger than depth (Figure 1;Talke et al., 2013). As observed in Fig. 1a, three slow patches (red coloring) of ~100 seconds duration (50m length scale) are bracketed by 100-150 second patches of much faster flow (75-100m scale). Slow patches are associated with upwards directed flow, while fast patches exhibit neutral or downwelling flow (Fig. 1c). Since the elevated temperature observed in boils is correlated with slow patches (Fig. 2a, 2b), quasi-2D features appear on the surface as agglomerations of many individual boils. Notably, neither divergence or vorticity show any large scale surface patterns beyond the boil size of 1-3m (Fig 2c,2d). The reason is simple: The surface boundary condition (no flow through surface) produces a 'blockage layer' which prevents upwelling (boiling) from occurring at scales roughly greater than the depth (Talke et al., 2013). Therefore, a single, width-scale boil cannot occur. Surface vorticity from IR-PIV data appears to be produced by shear between boils and boils/ambient flow, and is therefore limited by these scales (Fig 2d).

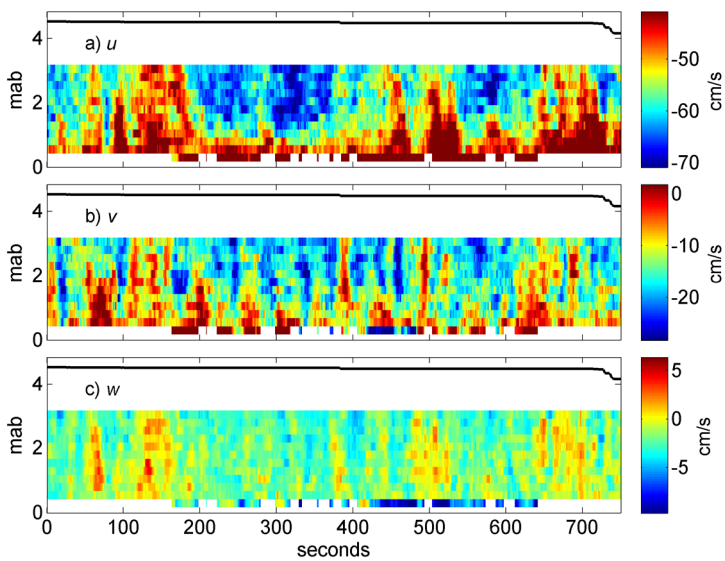

Figure 1: Along channel (a), cross channel (b), and vertical velocity (c) in the tidal Snohomish River during an ebbing tide on Sept. 24th, 2009. River depth was approximately 4m.

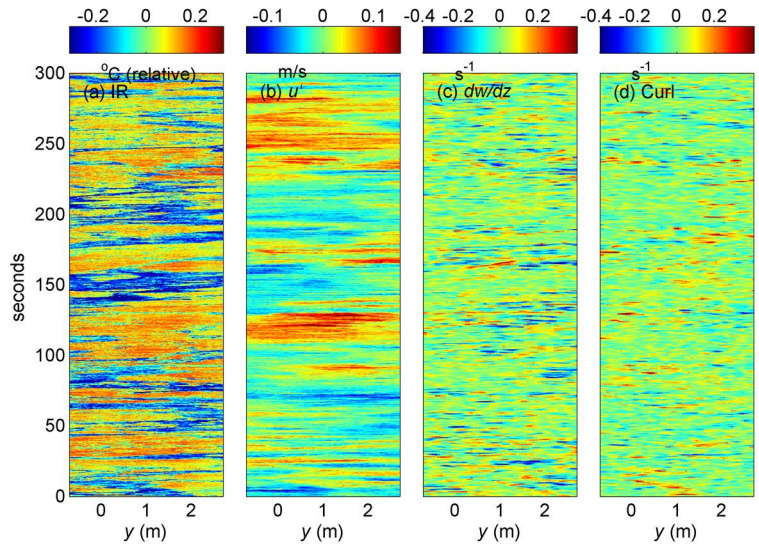

Figure 2: A time stack of surface temperature (a), along-channel velocity anomaly (b), divergence (c; dw/dz = -du/dx -dv/dy) and curl (d; vorticity) in the tidal Snohomish River on Sept. 24, 2009. The x-axis denotes the lateral (cross flow) direction. Velocity was estimated using a feature-following, particle image velocimetry (PIV) algorithm . Measurements and methods are described in Chickadel et al. (2011) and Talke et al. (2013).

The pattern of boil-agglomeration observed in the Snohomish (Fig. 1-2; Annual Report, 2012) is also observed in the Columbia River estuary (Figure 3a). Large (>50m) streaks of elevated thermal temperature (white) and cooler temperatures (black) are observed in the along-channel direction (Fig. 3a), and are much larger than the depth (~10-15m). Along channel spectra of IR images are more energetic for length scales greater than 60m (Fig. 4); this anisotropy occurs because thermal features show a tendancy to organize in boil streets (Fig. 3a). Interestingly, such boil streets are not observed everywhere (Fig. 3b), and shorter length scales and 'round' conditions occur where the river is wider, while the most elongated features occur at the sharpest bends and constrictions (Fig. 5). Thus, along-channel stretching of existing coherent structures due to flow acceleration may help explain the observed thermal anisotropy. River geometry and bedform influence may also produce more energetic boils in these locations. Interestingly, the spectral slope in Fig. 4 lies between the theorized $k^{-5/3}$ Kolmogorov cascade for 3D turbulence and a k^{-1} energy decrease. The k^{-1} cascade is anticipated for scalar spectra (i.e. temperature) for 2D turbulence [e.g. *Schorghofer*, 2000; *Kraichnan and Montgomery*, 1980]. The observed slope is therefore consistent with the intepretation that these boil fields may represent some intermediate state of turbulence between 2D and 3D.

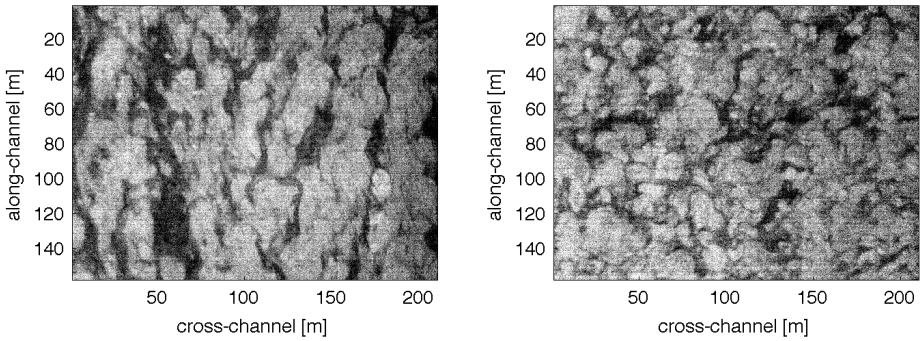

Figure 3. Examples surface thermal features in the tidal Columbia River from (left) near a bend and (right) along a straight channel section.

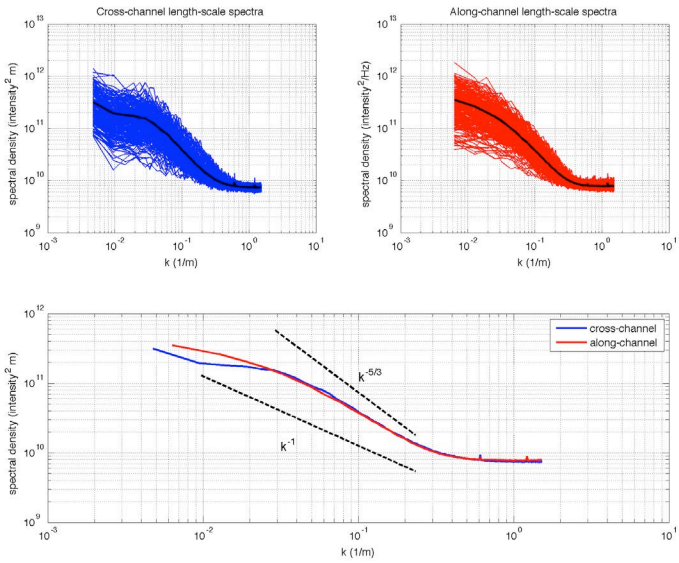

Figure 4. Wavenumber spectra of thermal imagery from 223 images in a 30 km section of the Columbia River between Cathlamet Bay and Wauna. Cross-channel ((top left) spectra and along-channel spectra (top right) show the dominance of large-scale features. Mean spectra are shown in black. Features larger than ~60m are stretched in the along-channel direction (bottom).

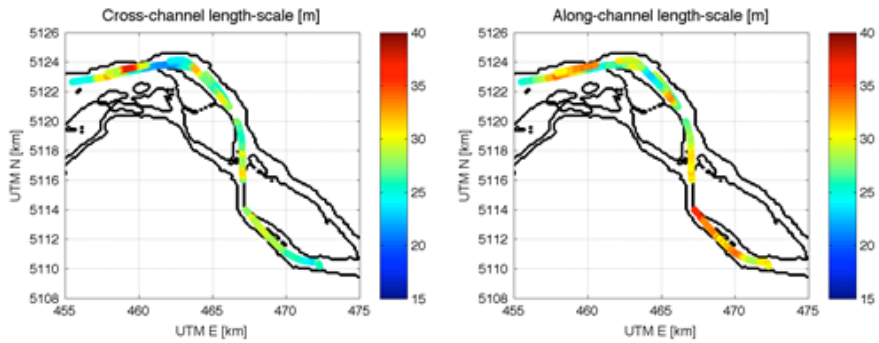

Figure 5. Maps of spectral energy weighted mean wavelengths for (left) cross-channel and (right) along-channel directions in the CRE. A representative boil scale was calculated as inverse of the energy weighted mean wavenumber.

Analysis of mouth of San Francisco Bay and Columbia: Shallow turbulent structures are also observed in surface waters at estuary mouths, but are unrelated to agglomerations of bottom-generated boils (Figs. 6-11). The map of surface temperature in Fig. 6 depicts 200m-scale eddies between Sand Island (E =422km) and Jetty A (E = 420km). The SAR derived vertical vorticity shows that alternating eddy motions directly correspond to surface temperature patterns: warm (freshwater) and cold (seawater) eddies alternate. Similar alternating patterns of positive and negative vorticity are also observed in a Delft 3D numerical model in the same (highly sheared) location (Fig. 7). In both measurements and model, a ribbon of vorticity (shear) is observed emanating in the northwest direction off the tip of Jetty A (Fig. 6&7). Topography, shear, and stratification clearly influence the observed patterns.

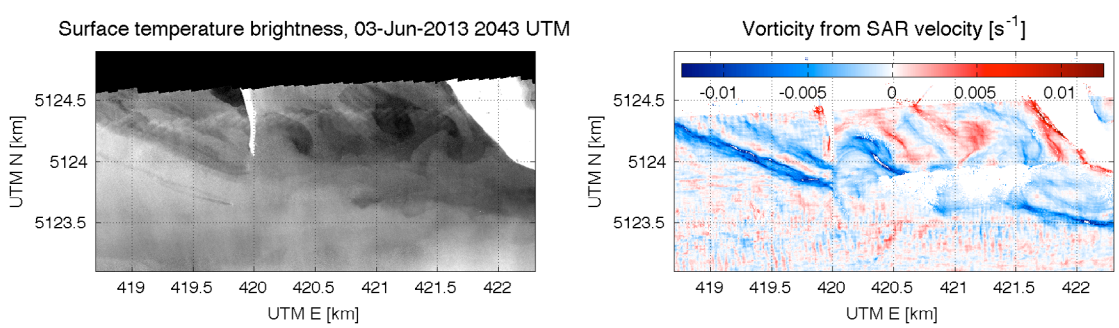

Figure 6. (above left) Surface brightness temperature mosaic near the mouth of the Columbia River (warmer is brighter) and (right) surface vertical vorticity derived from simultaneous airborne IR and SAR derived velocity, respectively. The ebb tide currents flow from east to west (right to left).

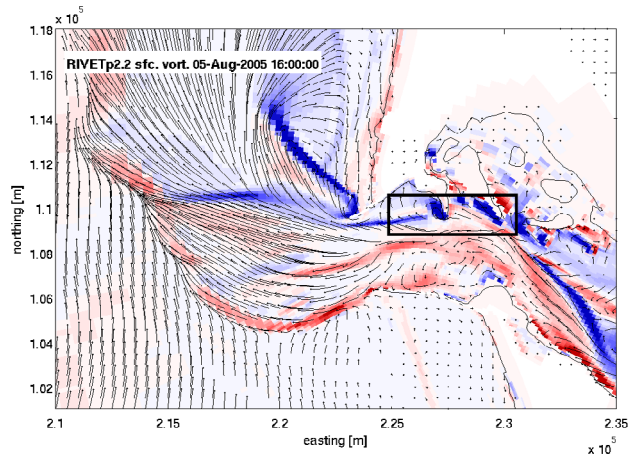

Figure 7: Modelled Vorticity at the mouth of the Columbia River during stratified conditions, with instantaneous streamlines overlaid. The Area of Fig. 6 approximated by the inlaid box. Peak vorticity is +/- 0.002 s^{-1}

Spectral analysis of the 2005 Megatransect moorings illustrate that much of the residual velocity variance (the shallow turbulence) is associated with the semidiurnal tidal variance in the channel (Fig. 8b & c), whereas the residual spectrum on the northern shelf is not as peaked near the tidal periods (Fig. 8a). Vertical variations in the residual kinetic energy spectra illustrate that the shallow turbulence becomes decoupled from the tides closer to the water surface. A dynamical interpretation of the Megatransect data suggests that tidal residual currents (mean currents driven by the divergence of the tidal Reynolds stress) contribute to the mean circulation on the northern shoal. Nonetheless, inspection of model simulations and analysis of the term balance suggests that the northward eddy flux of anticyclonic vorticity generated at the tip of Jetty A is significant (Fig. 9). Vorticity generation occurs via the torque of the bottom stress, which occurs where the mean current is transverse to the topographic gradient. The eddy viscosity estimated for shallow turbulence, 20 m^2/s, is the correct size to transport mean vorticity onto the northern shoal, where it is dissipated by the mean bottom stress.

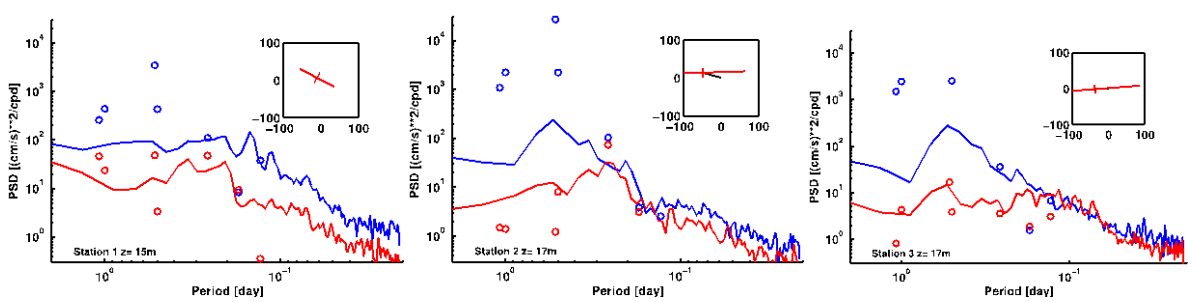

Figure 8 (above): Power spectra of near surface velocity in the Mouth of the Columbia River on the northern shoal (left), at the northern edge of the channel (middle), and mid-channel (right). Circles show spectral density associated with the tide, while curves show spectral density of the non-tidal residual velocity in a coordinate system aligned with the tidal ellipse (blue, major axis; red minor axis).

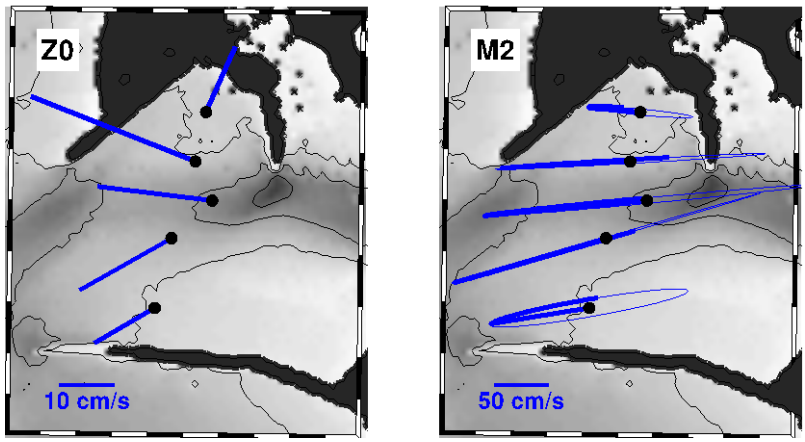

Figure 9 (left): Mean currents and M2 tidal ellipses at the Megatransect mooring sites. The northward component of the mean current at the northermost station can be explained as a rectified tidal current; however, the inclination of the tidal ellipses relative to the direction of the mean current indicates that the tidal Reynolds stress is in the wrong direction to drive anticyclonic vorticity on the northern shoal.

In San Francisco Bay, CODAR measurements show large eddies and vertical vorticity that (like the CRE) appear to scale with topographic features and/or width scales (Fig. 10). These rotational features are 'forced vortices' and are most prominent during slack tide, when vertical mixing is minimal. Such structures appear to be influenced by river flow conditions, as are other hydrodynamic properties at the estuary mouth (Fig. 11). As river flow increases during winter storm events (blue line, Fig. 11a), the M2 tidal amplitude and the major-axis M2 tidal velocity is reduced (green line and black line, Fig. 11a), the 2psu X2 isohaline moves downstream, and stratification increases (see also Moftakhari et al., 2013). These changes are correlated with an increase in the surface flow variance ("TKE"), after removing tidal and tidally-averaged flow patterns. Both "flow variance" and "dissipation" estimated from the integral lengthscale are correlated with river discharge, and are largest during peak flow (Fig. 11b). Further, the ratio of vorticity to divergence increases during the stormy period between day 150-200, suggesting that horizontal rotational motions are becoming more prominent, relative to vertical (dw/dz) processes. The cross-channel velocity gradient du/dy increases as well (not shown).

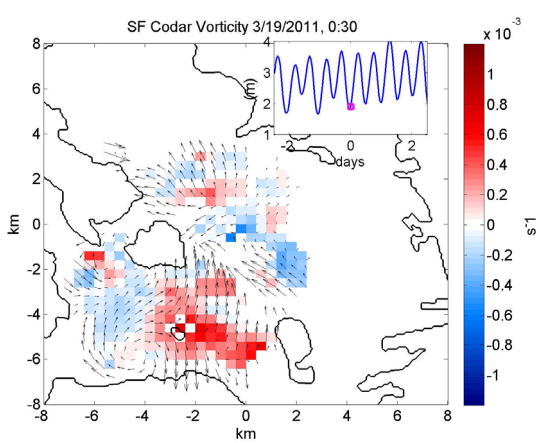

Figure 10 (left): Vorticity in SF Bay during a river freshet, estimated from CODAR velocity

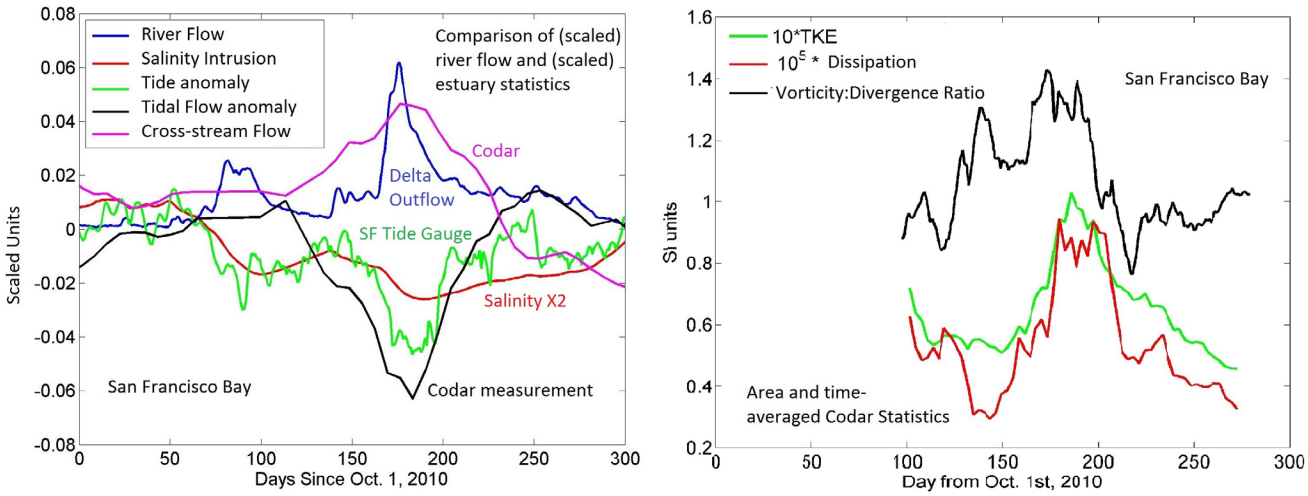

Figure 11 Time series of river discharge in SF Bay, M2 tidal admittance anomaly (deviation of measured from predicted tide, normalized by astronomic potential), M2 velocity anomaly (deviation from predicted tidal velocity) and X2 salinity intrusion (deviation from normal position of 2 psu isohaline). Right: Time series of TKE = $u'^2 + v'^2$, "dissipation", and the vorticity to divergence ratio.

Synthesis: The shallow turbulence evaluated here spanned a continuum of bottom-boundary influence. In the Snohomish tidal river, the shear stability number, $S = \frac{\varepsilon_{BBL}}{\varepsilon_{nD}} = \frac{WC_d}{H}$, where C_d = drag coefficient, W = width and H = depth, ranged from 0.05-0.4 (Uijttewaal & Booij, 2000; Uijttewaal & Jirka, 2003, within the shallow turbulence range. Conditions there (and in the tidal Columbia River) clearly support bottom boundary turbulence, as can be inferred from the presence of surface boiling. Flow statistics and visual images of boil streets show that such quasi-2D motions exist and are related to/caused by the tendancy of individual boils to organize into larger patterns. At the mouth of estuaries, greater depth and lower drag (due to stratification) increases the horizontal length-scale to which shallow turbulent eddies remain stable. Hence, eddies of >200m lengthscale are observed both in IR images, surface velocity maps, and in numerial models (Figs. 6-11). The effect of bottom boundary turbulence—as evidenced by less obvious boiling action and upwelling—is more muted. As river flow increases, increased variance (TKE) and "dissipation" is observed in surface flows, and vertical vorticity becomes prominent relative to divergence (upwelling). These observations suggest that large scale shallow turbulent motions become more prevalent as surface conditions become more stratified and unconnected to the bed (deeper).

IMPACT/APPLICATIONS

Impacts and applications of our work include:

1. Remotely-sensed turbulence features provide information about the underlying depth, velocity, stratification, and turbulent kinetic energy balance. Improved knowledge of these features can be used to help define and ground-truth models, by providing additional calibration data and by helping to determine appropriate vertical and spatial resolution (for example, to enable correct characterization of large scale eddy motions which can adjust tidal velocites by 20%).

2. Predictions of tides and currents in estuaries are often incorrect because conditions are non-stationary; Our analysis approach in SF Bay provides a template for quantifying and understanding how currents and tides vary as river flow and stratification change. In turn, this provides higher-order, time varying statistics (e.g., Fig. 11) against which to calibrate and verify models, which are typically only calibrated for mean-conditions.

3. Characterizing large-scale, quasi 2D turbulence helps elucidate the mechanisms by which energy is extracted from the mean tidal flow and is transferred between different scales. Understanding this process helps in the parameterization and validation of models.

RELATED PROJECTS

The ONR-sponsored "Young-Investigator" award for Talke aims to improve numerical models of transport by analyzing satellite data, primarily through scalars such as sediment, salinity, and temperature. There is therefore some synergy and cross-over, particularly in the analysis of CODAR data. LIDAR data collected along with Columbia River Thermal imagery (Figs. 3-6) is being analyzed for tidal signals under the auspices of the YIP award. The River Mouth and Inlet Dynamics (RIVET) DRI and the Data Assimilation for Remote Sensing Littoral Application (DARLA) MURI, both funded through ONR, have overlapping goals and research areas with this work. Specifically, the connection of turbulence length-scales and surface flow measured with remote sensing have allowed for added opportunities for data collection and analysis. This research will also benefit from a current ONR DURIP award ('Stabilized Gimbal for Airborne Water Surface Velocity Measurements in Riverine and Littoral Environments', Chickadel PI) to measure large-scale surface velocity and to identify turbulent features in surface temperature.

REFERENCES

Adrian, R.J., K.T. Christensen, Z.C.Liu, (2000). Analysis and interpretation of instantaneous turbulent velocity fields, *Experiments in Fluids* **29**, 275-290.

Anderson & Dugan, (2011). Surface Currents in Rivers and Estuaries derived from airborne IR remote sensing, Areté Associates pdf.

Chickadel, C. C., Talke, S. A., Horner-Devine, A. R., and Jessup, A. T. (2011). Infrared-based measurements of velocity, turbulent kinetic energy, and dissipation at the water surface in a tidal river. *Geoscience and Remote Sensing Letters, ,* GRSL-00530-2010.R1

Dugan, J. P. and Piotrowski, C. C. (2011). EO observations of currents and turbulence via mixing of sediment load variations. In *IEEE/OES 10th Current, Waves and Turbulence Measurement Conference* (CWTMC '11), Monterey, CA. IEEE.

Kraichnan, R. H., & D. Montgomery, 1980. Two-dimensional turbulence. Rep. Prog. Phys. (43), p. 547-619.

Moftakahri, H.R., D.A. Jay, S.A. Talke, T. Kulkulka, P. D. Bromirski, 2013. A novel approach to flow estimation in tidal rivers, *Water Resources Research*. 49, 1-16, doi:10.1002/wrcr.20363

Moritz, H. R., Gelfenbaum, G. R., and Ruggiero, P. (2005). Morphological implications of oceanographic measurements acquired along a mega-transect at the mouth of the Columbia River, USA. In *American Geophysical Union, Fall Meeting, pages OS23A–1534*. American Geophysical Union.

Schorghofer, N., 2000. Energy spectra of steady two-dimensional turbulent flows. *Physical Review E 61*, 6572-6577

Talke, S.A., A.R. Horner-Devine, C.C. Chickadel, and A. T. Jessup, 2013. Turbulent kinetic energy and coherent structures in a tidal river. *Journal of Geophysical Research.* 118(12), p. 6965–6981, DOI: 10.1002/2012JC008103

Uijttewaal, W.S.J., & R. Booij, 2000. Effects of shallowness on the development of free-surface mixing layers. *Physics of Fluids* **12(2)**, p. 392-401.

Uijttewaal, W.S.J., & G.H. Jirka, 2003. Grid turbulence in shallow flows, *J. Fluid Mechanics*, **489** p 325-344.

Zhou, H., R.J. Adrian, S. Balachandar (1996). Autogeneration of near wall vertical structures in channel flow. *Physics of Fluids* 8: 288-290.

Zaron, E.D., H.R. Moritz, and G.R. Gelfenbaum (2012). Characteristics of Shallow Turbulence in the Mouth of the Columbia River, talk presented at the 3rd International Symposium on Shallow Flows, University of Iowa, Iowa City, June 4-6.

PUBLICATIONS

Talke, S.A., A.R. Horner-Devine, C.C. Chickadel, and A. T. Jessup, 2013. Turbulent kinetic energy and coherent structures in a tidal river. *Journal of Geophysical Research.* 118(12), p. 6965–6981, DOI: 10.1002/2012JC008103 . [Published, refereed]

Jessup, A.T., Chickadel, C.C., Talke, S.A., and A.R. Horner-Devine, 2013. *COHSTREX: Coherent Structures in Rivers and Estuaries Experiment*. Ch. 14 in Coherent Flow Structures at the Earth's Surface (Editors J.G. Venditti, J.L.Best, M. Church, J.R. Hardy), John Wiley and Sons, New York. [Published]

HONORS/AWARDS/PRIZES

Outstanding Reviewer Award, Estuaries and Coasts, 2013 (Talke)

Outstanding Researcher Award, Sigma Xi (Portland Chapter), 2014 (Talke)

Faculty Research Excellence Award, Portland State University, 2014 (Zaron)